

## Response to Reviewer

Thank you for your commendation and appreciate your suggestions on all scientific, technical aspects of our article. The manuscript has been revised accordingly. Listed below is our point-to-point response to each comment.

### General comments:

The authors have sufficiently addressed the review comments though some revision is still necessary to add missing citations and also to improve the written English.

Response: We thank the reviewer for pointing out the grammatical errors and inappropriate expressions in the manuscript. We have revised them as suggestion.

### Specific comments:

1. Line 35: This is an unusual choice - Maria's paper is about global OA and climate.

Response: We thank the reviewer for reminding this. The sentence has been revised between Line 34 to Line 35: “Organic aerosols account for approximately 20-50 % of ambient fine particulate matter (PM<sub>2.5</sub>), with significant environment, climate and health effects (Maria et al., 2004; Kanakidou et al., 2005)”.

2. Line 43: Cite Zhao Bin's Scientific Reports 2016 paper here as it directly addresses SOA formation from vehicle IVOC emissions in China.

Response: Thanks for the suggestion. One sentence is added between Line 43 to Line 45: “Zhao et al. (2016) also reported that intermediate volatility organic compounds (IVOCs) from vehicles constituted a large percentage of SOA concentration in China by chamber experiments as well as the two-dimensional volatility basis set (2D-VBS) box model simulations”.

3. Line 253-256: This is the whole point of Donahue et al EST 2006. Please cite!

Response: We thank the reviewer for pointing out this. The sentence is modified as “High particle mass loadings are favorable for the partitioning of semi-volatile compounds into the particle phase, potentially increasing SOA mass yields (Odum et al., 1996; Donahue et al., 2006). Third, stronger partitioning of SOA precursors into the particle phase may reduce oxidation rate in the gas phase, which will potentially reduce the rate of SOA production (Seinfeld et al., 2003; Donahue et al., 2006)” between Line 255 to Line 259.

4. Line 262: What are C8 and C9 benzene? Is this TMB? Call them alkyl benzenes or something like that.

Response: Thanks for the suggestion. The C8 alkylbenzene includes ethylbenzene and o-, m-, p-xylene, and C9 alkylbenzene includes n-, i-propylbenzene, o-, m-, p-ethyltoluene, and 1,2,3-, 1,2,4-, 1,3,5-trimethylbenzene. They are added between Line 265 to Line 267:

“In this study, benzene, toluene, C8 alkylbenzene (e.g., ethylbenzene and o-, m-, p-xylene) and C9 alkylbenzene (e.g., n-, i-propylbenzene, o-, m-, p-ethyltoluene, and 1,2,3-, 1,2,4-, 1,3,5-trimethylbenzene)...”.

#### Reference

Donahue, N. M., Robinson, A. L., Stanier, C. O., and Pandis, S. N.: Coupled partitioning, dilution, and chemical aging of semivolatile organics, *Environ. Sci. Technol.*, 40, 2635-2643, 10.1021/es052297c, 2006.

Maria, S. F., Russell, L. M., Gilles, M. K., and Myneni, S. C. B.: Organic aerosol growth mechanisms and their climate-forcing implications, *Science*, 306, 1921-1924, 10.1126/science.1103491, 2004.

Zhao, B., Wang, S., Donahue, N. M., Jathar, S. H., Huang, X., Wu, W., Hao, J., and Robinson, A. L.: Quantifying the effect of organic aerosol aging and intermediate-volatility emissions on regional-scale aerosol pollution in China, *Scientific Reports*, 6, 10.1038/srep28815, 2016.

# 1 **Comparison of primary aerosol emission and secondary aerosol formation from gasoline direct injection and** 2 **port fuel injection vehicles**

3 Zhuofei Du<sup>1</sup>, Min Hu<sup>1,3\*</sup>, Jianfei Peng<sup>1†</sup>, Wenbin Zhang<sup>2</sup>, Jing Zheng<sup>1</sup>, Fangting Gu<sup>1</sup>, Yanhong Qin<sup>1</sup>, Yudong Yang<sup>1</sup>,  
4 Mengren Li<sup>1</sup>, Yusheng Wu<sup>1</sup>, Min Shao<sup>1</sup>, Shijin Shuai<sup>2</sup>

5 1. State Key Joint Laboratory of Environmental Simulation and Pollution Control, College of Environmental  
6 Sciences and Engineering, Peking University, Beijing 100871, China

7 2. State Key Laboratory of Automotive Safety and Energy, Department of Automotive Engineering, Tsinghua  
8 University, Beijing 100084, China

9 3. Beijing Innovation Center for Engineering Sciences and Advanced Technology, Peking University, Beijing  
10 100871, China

11 † Now at Department of Atmospheric Sciences, Texas A&M University, College Station, TX 77843, US

12

13 \*Corresponding author: Min Hu, minhu@pku.edu.cn

14

15

## 16 **Abstract**

17 Gasoline vehicles **significantly** contribute to urban particulate matter (PM) pollution. Gasoline direct injection (GDI)  
18 engines, known as their higher fuel efficiency than that of port fuel injection (PFI) engines, have been increasingly  
19 employed in new gasoline vehicles. However, the impact of this trend on air quality is still poorly understood. Here,  
20 we investigated both primary emissions and secondary organic aerosol (SOA) formation **from a GDI and a PFI**  
21 **vehicle under an urban-like driving condition**, using combined approaches involving chassis dynamometer  
22 measurement and environmental chamber simulation. The PFI vehicle emits slightly more volatile organic  
23 compounds, e.g., benzene and toluene, whereas the GDI vehicle emits more particulate components, e.g., the total  
24 PM, elemental carbon, primary organic aerosols and polycyclic aromatic hydrocarbons. Strikingly, **we found** a  
25 much higher SOA production (by a factor of approximately 2.7) from the exhaust of the GDI vehicle than that of

26 the PFI vehicle under the same conditions. More importantly, the higher SOA production found in the GDI vehicle  
27 exhaust occurs concurrently with lower concentrations of traditional SOA precursors, e.g., benzene and toluene,  
28 indicating a greater contribution of intermediate volatility organic compounds and semivolatile organic compounds  
29 in the GDI vehicle exhaust to the SOA formation. Our results highlight the considerable potential contribution of  
30 GDI vehicles to urban air pollution in the future.

31

32

### 33 **1 Introduction**

34 Organic aerosols (OAs) account for approximately 20-50 % of ambient fine particulate matter (PM<sub>2.5</sub>), **with**  
35 **significant environment, climate and health effects** (Maria et al., 2004; Kanakidou et al., 2005). Primary organic  
36 aerosol (POA) is emitted directly by sources, while secondary organic aerosol (SOA) is mainly formed via  
37 oxidation of gaseous precursors in the atmosphere and account for about 30-90 % of the OA mass worldwide  
38 (Zhang et al., 2007; Hu et al., 2016), but SOA source remain poorly constrained. Robinson et al. (2007) proposed  
39 that low-volatility gas-phase species emitted from diesel vehicles were important sources for urban ambient SOA,  
40 which achieved better mass closure between observed and modeled SOA. Using an updated CMAQ model, Jathar  
41 et al. (2017) found that 30-40% OA was contributed from vehicles in the southern California, and half of which  
42 was SOA. Huang et al. (2014) recently revealed that 15-65 % of SOA was contributed by fossil fuel consumption  
43 (i.e., traffic and coal burning) in megacities in China. **Zhao et al. (2016) also reported that intermediate volatility**  
44 **organic compounds (IVOCs) from vehicles constituted a large percentage of SOA concentration in China by**  
45 **chamber experiments as well as the two-dimensional volatility basis set (2D-VBS) box model simulations.** These  
46 findings indicated that vehicles have important contribution to ambient SOA in urban areas. An ambient organic  
47 aerosol measurement in the Los Angeles Basin demonstrated that SOA contributed from gasoline vehicles was  
48 significant in the urban air, much larger than that from diesel vehicles (Bahreini et al., 2012). **A similar** conclusion  
49 was reached by Hayes et al. (2013) based on mass spectrometer results. Meanwhile, several chamber simulation  
50 studies concluded that **the** exhaust of gasoline vehicles could form substantial SOA (Jathar et al., 2014). Thus,

51 **gasoline vehicle exhaust** is highly associated with ambient SOA formation.

52 Gasoline vehicles can be categorized into two types based on the fuel injection technologies in their engines,  
53 i.e., port fuel injection (PFI) vehicles and gasoline direct injection (GDI) vehicles. Unlike a PFI engine, in which  
54 gasoline is injected into intake port, gasoline is sprayed into cylinder directly in a GDI engine. With the increased  
55 atomization and vaporization rate of fuel, and more accurate control of fuel volume and injection time, a GDI  
56 engine has many advantages, such as better fuel efficiency, lower CO<sub>2</sub> emissions and less fuel pumping loss  
57 (Alkidas, 2007; Myung et al., 2012; Liang et al., 2013). In past decades, PFI vehicles dominated the market share  
58 of gasoline cars in the world. However, in recent years, GDI vehicles have been increasingly employed, due to their  
59 higher fuel efficiency. The market share of GDI vehicles in sales in 2016 reached about 25 %, 50 % and 60 % in  
60 China, the US and Europe, respectively (Wen et al., 2016; Zimmerman et al., 2016).

61 Several previous studies investigated the emissions of GDI and PFI vehicles, in terms of concentrations of  
62 gaseous pollutants, particle numbers and mass concentrations, and evaluated the reduction of emissions **with**  
63 **upgrading emission standards** (Ueberall et al., 2015; Zhu et al., 2016; Saliba et al., 2017). These studies showed  
64 that GDI vehicles emitted more primary particles than PFI vehicles (Zhu et al., 2016; Saliba et al., 2017), and even  
65 diesel vehicles equipped with **a diesel particulate filter (DPF)** (Wang et al., 2016). **These higher primary particle**  
66 **emissions are likely due to insufficient time allowed for gasoline fuel to be mixed with air thoroughly, as well as**  
67 **gasoline droplets impinging onto pistons and surfaces of combustion chamber in GDI engine** (Chen et al., 2017;  
68 Fu et al., 2017). **However, in most studies, vehicles were tested under the driving cycles of the US or European**  
69 **standards; those results may not representative of China's traffic conditions.**

70 SOA production from gasoline vehicle exhaust was previously simulated in smog chambers and potential  
71 aerosol mass (PAM) flow reactors. SOA formed from gaseous pollutants exceeds the related POA emissions and  
72 has much more contribution to air quality degradation. These studies mostly focused on the impacts of SOA  
73 formation by the model year (Gordon et al., 2014; Jathar et al., 2014; Liu et al., 2015), fuel formulations (Peng et  
74 al., 2017), driving cycles (including idling) (Nordin et al., 2013; Platt et al., 2013) and start-up modes of the gasoline  
75 vehicles (Nordin et al., 2013). Few studies, however, have investigated SOA formation from vehicles with different

76 engine technologies (GDI and PFI) under the same working condition.

77 In this study, both primary emissions and secondary aerosol formation from GDI and PFI vehicles were  
78 investigated. To represent typical urban driving patterns in megacities such as Beijing, the tested vehicles used  
79 gasoline fuel meeting the China Phase V fuel standard, and were operated over the cold-start Beijing cycle (BJC).  
80 The SOA formation from both the PFI and GDI vehicle exhausts were then simulated using a smog chamber.  
81 Finally, the overall contributions of the GDI and PFI gasoline vehicles to ambient particulate matter (PM) were  
82 evaluated. This study is part of a project that investigates the relationship between vehicle (engine) emissions and  
83 ambient aerosols, including potential of SOA formation from a PFI engine (Du et al., 2017) and the effects of  
84 gasoline aromatics on SOA formation (Peng et al., 2017).

85

## 86 **2 Materials and methods**

### 87 **2.1 Vehicles**

88 One PFI vehicle and one GDI vehicle were tested in this study to investigate their primary emissions and **SOA**  
89 **formation**. **The** vehicles were certified to the China Phase IV Emissions Standard (equivalent to Euro IV) and the  
90 China Phase V Emissions Standard (equivalent to Euro V), respectively. More information of the vehicles is shown  
91 in Table 1. The fuel used in the experiments was a typical Phase V gasoline on the China market (sulfur content =  
92 6 mg kg<sup>-1</sup>). More information **on** the fuel is provided in Table S1 in the Supplement. Cold-start BJC, characterized  
93 by a higher proportion of idling periods and lower acceleration speeds than the New European Driving Cycle  
94 (NEDC), was performed to simulate the repeated braking and acceleration on road in megacities such as Beijing.  
95 The BJC lasted for approximately 17 minutes, with a maximum speed of 50 km h<sup>-1</sup> (Peng et al., 2017).

96

### 97 **2.2 Experimental setup**

98 The chamber experiments were carried out in the summer at the State Key Laboratory of Automotive Safety  
99 and Energy of Tsinghua University in Beijing, including two experiments conducted with the GDI vehicle and four  
100 experiments conducted with the PFI vehicle. The tested vehicles were placed on a chassis dynamometer system

101 (Burke E. Porter Machinery Company) with a controlled room temperature of  $26.4 \pm 2.5$  °C and absolute humidity  
102 of  $11.5 \pm 2.4$  g m<sup>-3</sup>. The exhaust emitted by the vehicle tailpipe was diluted in a constant volume sampler (CVS)  
103 system, where the flowrate was maintained at 5.5 m<sup>3</sup> min<sup>-1</sup> using filtered ambient air, achieving about 20-fold  
104 dilution of the exhaust. Several instruments, including an AVL CEBII gas analyzer, a Combustion Differential  
105 Mobility Spectrometer (DMS500) and a particle sampler, were connected to the CVS (detailed in Figure 1 and  
106 section 2.3) to characterize the primary gas- and particulate-phase pollutants. The diluted exhaust produced by the  
107 CVS system was injected into an outdoor chamber, where secondary aerosol formation was simulated. This was  
108 the second dilution step of the exhaust with a dilution factor of approximately 15. A schematic illustration of the  
109 outdoor experimental setup is shown in Figure 1.

110 The photochemical oxidation experiments were carried out in a quasi-atmospheric aerosol evolution study  
111 (QUALITY) outdoor chamber. More details of the setup and performance of the QUALITY chamber were  
112 introduced by Peng et al. (2017). Prior to each experiment, the chamber was covered with a double-layer anti-  
113 ultraviolet (anti-UV) shade to block sunlight and was cleaned with zero air for about 15 h to create a clean  
114 environment. Approximately 120 ppb O<sub>3</sub> were injected into the chamber prior to the injection of the vehicle exhaust  
115 to make the oxidation environment similar to the mean O<sub>3</sub> peak concentration in the ambient atmosphere. Before  
116 the chamber was exposed to sunlight, about 15-minute period was left to ensure that the pollutants were mixed  
117 sufficiently in the chamber, then the initial concentrations were characterized in the dark. Subsequently, the anti-  
118 UV shade was removed from the chamber and photo-oxidation was initiated. A suite of high time resolution  
119 instruments was utilized to track the evolution of pollutants during the chamber experiments. Zero air was added  
120 into the chamber during sampling period to maintain a constant pressure.

121

## 122 2.3 Instrumentation

123 Primary gases and aerosols were measured by the instruments connected to the CVS. The concentrations of  
124 gaseous pollutants, including CO, CO<sub>2</sub>, NO<sub>x</sub> and total hydrocarbon (THC) were monitored with a gas analyzer  
125 AVL Combustion Emissions Bench II (CEB II, AVL, Austria). Primary aerosols were measured with both on-line

126 and off-line instruments. A DMS500 (Cambustion, UK) was implemented to monitor the real-time number size  
127 distribution and total number concentration of primary particles. Its sampling line was heated to maintain the  
128 temperature at 150°C. The aerosols were also collected on Teflon and quartz filters by AVL Particulate Sampling  
129 System (SPC472, AVL, Austria) to analyze the mass, organic carbon (OC) and elemental carbon (EC) emission  
130 factors using a balance and an OC/EC analyzer (Sunset Lab, USA).

131 During the chamber experiments, a suite of real-time instruments was utilized to characterize the **evolution** of  
132 the gas and particulate-phase pollutants. **A CO analyzer, a NO-NO<sub>2</sub>-NO<sub>x</sub> analyzer and an O<sub>3</sub> analyzer** (Thermo  
133 Fisher Scientific Inc., USA) were employed to measure the concentrations of CO, NO<sub>x</sub> (including NO and NO<sub>2</sub>)  
134 and O<sub>3</sub>, respectively. **The evolution of volatile organic compounds (VOCs) was monitored with a proton transfer**  
135 **reaction mass spectrometer** (PTR-MS, IoniconAnalytik, Austria) (Lindinger et al., 1998). H<sub>3</sub>O<sup>+</sup> was used as the  
136 reagent ion, which reacted with the target compounds. The resulting ions were detected by a quadruple mass  
137 spectrometer. Meanwhile, the particles size distribution was characterized using a scanning mobility particle sizer  
138 system (SMPS, TSI, USA), which consisted of a differential mobility analyzer (DMA, TSI, USA) and a  
139 condensation particle counter (CPC, TSI, USA). **This system can measure aerosols with diameters ranging from 15**  
140 **nm to 700 nm.** A high-resolution time-of-flight aerosol mass spectrometer (HR-Tof-AMS, Aerodyne Research,  
141 USA) **was used** to obtain mass concentrations and size distributions of submicron, non-refractory aerosols,  
142 including sulfate, nitrate, ammonium, chloride and organic (DeCarlo et al., 2006). Table 2 lists the instruments used  
143 to measure the primary emissions and their evolutions in the chamber experiments.

144

## 145 **3 Results**

### 146 **3.1 Primary emissions**

#### 147 **Gaseous pollutant emissions**

148 Emission factors (EFs) of CO<sub>2</sub>, THC, benzene and toluene from the GDI and PFI vehicles are listed in Table  
149 3. The EFs of CO<sub>2</sub> and THC are derived from measured concentrations in CVS, while the EFs of benzene and  
150 toluene were calculated from the initial concentrations in the chamber. The THC emission factor was reported in



151 units of carbon mass,  $\text{g C kg}^{-1}\text{fuel}^{-1}$ .

152 The GDI vehicle emitted less  $\text{CO}_2$  and THC than the PFI vehicle due to their different fuel injection strategies  
153 and mixing features (Liang et al. 2013; Gao et al., 2015). The EF of THC from the GDI vehicle met the standard  
154 of the China Phase V Emission Standard ( $0.1 \text{ g km}^{-1}$ ), but that from the PFI vehicle was slightly above the standard  
155 limit. The PFI vehicle used in this study met a less stringent emission standard (the China Phase IV), which might  
156 cause additional THC emissions when compared to the China Phase V Emission Standard. In addition, in this study  
157 we employed the BJC whereas the standard is based on the NEDC. More repeated braking and acceleration in the  
158 BJC (Figure S2) might cause incomplete combustion and consequently higher THC emission from the PFI vehicle.  
159 As typical VOC species emitted by vehicles, benzene and toluene were measured in this study. For both vehicles,  
160 the EFs of toluene were higher than those of benzene. Consistent with the feature of THC emission, the PFI vehicle  
161 emitted more benzene and toluene than the GDI vehicle, and the enhancement of toluene was much larger than that  
162 of benzene.

163 The EFs of the gaseous pollutants in this study had similar magnitudes to those in previous studies in which  
164 gasoline vehicles met comparable levels of emission standards and were tested under cold-start driving condition,  
165 while the results in this study were slightly higher, as shown in Table 3. This difference might be because the  
166 California ultralow-emission vehicles (ULEV) (Saliba et al., 2017) and most LEV II vehicles (manufactured in  
167 2004 or later) (May et al., 2014) meet the US certification gasoline emission standards for the ULEV category,  
168 which has a lower limit of gaseous pollutants than the China Phase V Emission Standard. In addition, the different  
169 driving cycles of our study from those other studies (listed in Table 3) might be another explanation for the  
170 difference in the EFs of gaseous pollutants.

### 171 **Primary particle emissions**

172 The EFs of PM, elemental carbon (EC), POA and particulate polycyclic aromatic hydrocarbons (PAHs) are  
173 shown in Table 4. The EF of  $\text{PM}_{2.5}$  from the GDI vehicle was about 1.4 times higher than that of the PFI vehicle.  
174 Both vehicles met the China Phase V Emission Standard for PM emission ( $4.5 \text{ mg km}^{-1}$ ). The GDI vehicle emitted  
175 about 3.3 times more EC and 1.2 times more POA than the PFI vehicle. The primary carbonaceous aerosols

176 (EC+POA) accounted for 85 % and 82 % of the PM in the GDI and PFI vehicles respectively, suggesting that  
177 carbonaceous aerosols were the major components in the PM from gasoline vehicles, especially for the GDI vehicle.

178 PAHs account for a small fraction of particulate organic matter in the atmosphere, but the molecular signature  
179 of PAHs can be utilized in source identification of vehicle emissions (Kamal et al., 2015). The GDI vehicle emitted  
180 about 1.5 times the PAHs of the PFI vehicle. The EFs of PAH compounds are listed in Table S2 in the Supplement,  
181 and the details of PAHs measurement were described in Li et al. (2016). It should be noted that the PAHs were  
182 tested under warm-start cycles. A higher EF of PAHs would be obtained under a cold-start cycle, since the lower  
183 temperature would lead to inefficient catalyst at the beginning of cold-start (Mathis et al., 2005). The main  
184 contributors to the total PAH mass emitted from gasoline vehicle exhaust in this study, especially from the GDI  
185 vehicle exhaust, were similar with the results reported by previous studies (Schauer et al., 2002; Hays et al., 2013).

186 The lower PM<sub>2.5</sub> and POA emissions from GDI vehicle were found in previous studies, except that a little  
187 higher PM<sub>2.5</sub> emission from GDI vehicle was illustrated in Saliba's study (Platt et al., 2013; May et al., 2014; Zhu  
188 et al., 2016; Saliba et al., 2017). The EC emissions were in the range of those of previous studies but on the lower  
189 level. The EF of the POA measured in this study was higher than those of other studies, leading to a higher OC/EC  
190 ratio, which could be attributed to the less strict emission standard of our vehicles and the different driving cycles  
191 applied in the experiments.

192 The bimodal number size distributions of the primary PM from the vehicles measured by the DMS500 are  
193 shown in Figure 2. The particle distributions of the exhaust of the GDI and PFI vehicles illustrated similar patterns,  
194 with two peaks located at about 10 nm for nucleation mode and at 60-90 nm for accumulation mode, respectively,  
195 which are consistent with the results of previous studies (Maricq et al., 1999; Chen et al., 2017). The particle  
196 number size distribution of the exhaust of the GDI vehicle showed a similar pattern to that of the PFI vehicle, with  
197 a much higher number concentration that is consistent with the emission of more particle mass.

198

### 199 **3.2 SOA formation from gasoline vehicle exhaust**

200 The time-resolved concentrations of gases and particles during the chamber experiments are illustrated in

201 Figure 3. Before removing the anti-UV shade, the initial concentrations of NO<sub>x</sub>, benzene and toluene from the PFI  
202 and GDI vehicles were 80 ppb, 3 ppb, 5 ppb and 100 ppb, 4 ppb, 14 ppb respectively.

203 After the aging experiment started (t=0 in Figure 3), NO was formed from NO<sub>2</sub> photolysis, and then reacted  
204 with O<sub>3</sub> to form NO<sub>2</sub>. The O<sub>3</sub> concentration increased rapidly to a maximum within 2-3 h and then decreased via  
205 reactions and dilution. Benzene and toluene decayed at different rates during the aging process.

206 New particle formation was found inside the chamber 15 minutes after the exhaust was exposed to sunlight,  
207 providing substantial seeds for secondary aerosol formation. **Significant growth of particles in both size and mass**  
208 **was observed in the chamber**, indicating that a large amount of secondary aerosol was formed during the  
209 photochemical oxidation. **The chemical composition of the secondary aerosols was measured continuously by a**  
210 **HR-ToF-AMS**. Organic was the dominant composition of the secondary aerosol, accounting for 88-95 % of the  
211 total particle mass inside the chamber (Figure S1), which is consistent with our previous research (Peng et al.,  
212 2017). The SOA mass exhibited different growth rate for the two types of vehicles. After a 4 h oxidation in the  
213 chamber, the SOA formed from the exhaust of the GDI vehicle was approximately double that of the PFI vehicle.

214 The solar radiation conditions significantly influenced the SOA formation. Thus, OH exposure was used to  
215 characterize the photochemical age as a normalization, instead of the experiment time. Two VOC species with  
216 noticeable differences in their reaction rate constants with OH radicals could be utilized to calculate the OH  
217 exposure ([OH] Δt) based on Equation 1 (for benzene and toluene, as used in this study) (Yuan et al., 2012).

$$218 \quad [\text{OH}] \Delta t = \frac{1}{k_T - k_B} \times \left( \ln \frac{[T]}{[B]} \Big|_{t=0} - \ln \frac{[T]}{[B]} \right) \quad (1)$$

219 where  $k_T$  and  $k_B$  are the OH rate constants of benzene ( $1.2 \times 10^{-12} \text{ cm}^3 \text{ molecule}^{-1} \text{ s}^{-1}$ ) (Yuan et al., 2012) and toluene  
220 ( $5.5 \times 10^{-12} \text{ cm}^3 \text{ molecule}^{-1} \text{ s}^{-1}$ ) (Kramp and Paulson, 1998), respectively.  $\frac{[T]}{[B]} \Big|_{t=0}$  is the concentration ratio of  
221 toluene to benzene at the beginning of the aging process, and  $\frac{[T]}{[B]}$  is their concentration ratio measured during  
222 aging process.

223 The SOA concentrations as a function of OH exposure are illustrated in Figure 4. Wall-loss correction and  
224 dilution correction, including both particles and gaseous pollutants, were taken into consideration in the calculation

225 of the SOA mass concentration in the chamber. Detailed descriptions of corrections are given in the Supplement.  
226 Assuming the mean OH concentration was  $1.6 \times 10^6$  molecular  $\text{cm}^{-3}$  in Beijing (Lu et al., 2013), the whole aging  
227 procedure in the chamber experiments was equal to a 6-10 h atmospheric photochemical oxidation. The average  
228 SOA concentrations were  $9.25 \pm 1.80$  and  $4.68 \pm 1.32$   $\mu\text{g m}^{-3}$  for the GDI and PFI vehicles, respectively, when the  
229 OH exposure was  $5 \times 10^6$  molecular  $\text{cm}^{-3}$  h in the chamber. Considering the driving cycle mileage and fuel  
230 consumption, the SOA productions were  $54.77 \pm 10.70$   $\text{mg kg}^{-1}$  fuel $^{-1}$  or  $3.06 \pm 0.60$   $\text{mg km}^{-1}$  for the GDI vehicle and  
231  $20.57 \pm 5.82$   $\text{mg kg}^{-1}$  fuel $^{-1}$  or  $1.55 \pm 0.44$   $\text{mg km}^{-1}$  for the PFI vehicle. Compared with the PFI vehicle, the GDI vehicle  
232 exhaust exhibited a higher potential of SOA formation, even though the PFI vehicle emitted more VOCs, which  
233 are considered as dominant classes of SOA precursors. This result indicates that higher concentrations of some  
234 other SOA precursors exist in the exhaust of GDI vehicles, which will be further discussed in section 3.3.

235 The results from chamber simulation of SOA formation from individual gasoline vehicles are illustrated in  
236 Figure 5. The SOA production from the both vehicles in this study is in the range of the results of previous studies  
237 (Nordin et al., 2013; Platt et al., 2013; Jathar et al., 2014; Liu et al., 2015; Peng et al., 2017). The variation of the  
238 SOA production among these studies might be caused by several factors: the model years of vehicles  
239 (corresponding to emission standards) (Nordin et al., 2013; Liu et al., 2015), their driving cycles (Nordin et al.,  
240 2013), the initial concentrations of gaseous pollutants in the chamber (Jathar et al., 2014), and the ratio of VOCs to  
241  $\text{NO}_x$  (Zhao et al., 2017) in the chamber experiments.

242 To investigate the dominant contributors to ambient PM from the GDI and PFI vehicles, Figure 6 illustrates  
243 the EFs of EC and POA as well as the production factors of SOA in this study. The SOA production from the GDI  
244 vehicle was approximately 2.7 times higher than that from the PFI vehicle. At  $5 \times 10^6$  molecular  $\text{cm}^{-3}$  h OH exposure,  
245 the SOA/POA ratio was close to unity. Figure 4 illustrates that the SOA production increased with photochemical  
246 age rapidly (within  $2 \times 10^7$  molecular  $\text{cm}^{-3}$  h). Thus, SOA would exceed POA at higher OH exposure, e.g., the  
247 SOA/POA ratio reached about 4 at  $10^7$  molecular  $\text{cm}^{-3}$  h OH exposure, becoming the major PM contributor. In  
248 terms of the POA and EC emissions as well as the SOA formation, the GDI vehicle contributed 2.2 times more  
249 than the PFI vehicle.

250 Although particle wall-loss correction as well as particle and gas dilution corrections were considered in this  
251 study, several factors may still contribute to the uncertainties of the SOA production. First, the loss of semi-volatile  
252 vapors to the chamber walls was not corrected, which may result in an underestimation of the rate of SOA  
253 production with a factor of 1.1-4.1 (Zhang et al., 2014). Second, under some ambient conditions such as severe  
254 urban haze events (Guo et al., 2014), particle mass concentrations can be as high as 200-300  $\mu\text{g m}^{-3}$ , much higher  
255 than the  $23 \pm 6 \mu\text{g m}^{-3}$  under the chamber conditions of this study. High particle mass loadings are favorable for  
256 the partitioning of semi-volatile compounds into the particle phase, potentially increasing SOA mass yields (Odum  
257 et al., 1996; Donahue et al., 2006). Third, stronger partitioning of SOA precursors into the particle phase may  
258 reduce oxidation rate in the gas phase, which will potentially reduce the rate of SOA production (Seinfeld et al.,  
259 2003; Donahue et al., 2006).

260

### 261 3.3 SOA mass closure

262 SOA production ( $\Delta\text{OA}_{\text{predicted}}$ ) estimated from VOC precursors can be defined as Eq. (2):

$$263 \Delta\text{OA}_{\text{predicted}} = \sum_i (\Delta_i \times Y_i) \quad (2)$$

264 where  $\Delta_i$  is the concentration change of precursor  $\text{VOC}_i$  measured with PTR-MS in the chamber experiments, and  
265  $Y_i$  is the SOA yield of the  $\text{VOC}_i$ . In this study, benzene, toluene, C8 alkylbenzene (e.g., ethylbenzene and o-, m-,  
266 p-xylene) and C9 alkylbenzene (e.g., n-, i-propylbenzene, o-, m-, p-ethyltoluene, and 1,2,3-, 1,2,4-, 1,3,5-  
267 trimethylbenzene) were involved in the estimation of SOA production, and alkanes and alkenes were not  
268 considered. A recent study found that ozonolysis of alkenes from gasoline vehicle exhaust could form SOA  
269 through aldol condensation reactions (Yang et al., 2018). However, much low declines of concentrations were  
270 observed than those of aromatics during chamber experiments, so alkenes might not play significant role in SOA  
271 formation in this study.

272 The SOA yield is sensitive to the VOCs/ $\text{NO}_x$  ratio (Song et al., 2005). In this study, the VOCs/ $\text{NO}_x$  ratio was  
273 in the range of 0.5-1.0 ppbC/ppb, thus, the SOA formation from the vehicle exhaust was determined under high  
274  $\text{NO}_x$  conditions. The high  $\text{NO}_x$  SOA yields of benzene and toluene were taken from Ng et al. (2007). The C8 and

275 **C9 alkylbenzenes** used the SOA yield of m-xylene from Platt et al. (2013).

276 The increased predicted SOA contribution from the VOC precursors as a function of OH exposure  
277 accumulation is demonstrated in Figure 7. At the end of the experiments, the SOA estimated from these speciated  
278 VOCs accounted for about 25 % and 53 % of the measured SOA formation from the GDI and PFI vehicle exhausts,  
279 respectively. Similar to the results of previous studies (Platt et al., 2013; Nordin et al., 2013; Gordon et al., 2014),  
280 single-ring aromatics play an important role in the SOA formation, especially for the PFI vehicle which shows  
281 higher predicted SOA fraction.

282 The unpredicted fraction of the measured SOA in the chamber experiments was in the range of 47-75 %.  
283 Contributions from **IVOCs** and semivolatile organic compounds (SVOCs), e.g., long branched and cyclic alkanes  
284 and gas-phase polycyclic aromatic hydrocarbons could be a possible explanation for this underestimation. The SOA  
285 formed by oxidation of IVOCs and SVOCs is found to dominate over that from single-ring aromatics (Robinson et  
286 al., 2007; Zhao et al., 2016). The unpredicted SOA ratio exhibited a maximum value at the beginning of the  
287 experiment, indicating that the IVOCs and SVOCs with low volatilities produced SOA much more efficiently than  
288 the single-ring aromatics with high volatilities, as the first generation products of photo-oxidation of these  
289 precursors form SOA (Robinson et al., 2007).

290 The larger fraction of the unpredicted SOA from the GDI vehicle exhaust might be associated with higher  
291 IVOCs and SVOCs emissions. Gas-phase PAH is one of the main component of speciated IVOCs (Zhao et al.,  
292 2016). The particulate-phase PAHs from the GDI vehicle were more abundant than those from the PFI vehicle by  
293 a factor of 1.5 (section 3.1). Based on gas-particle equilibrium, this indicates that more gas-phase PAHs, including  
294 some aromatic IVOCs, might be emitted by the GDI vehicles, which contribute to the SOA enhancement.

295

#### 296 **4 Discussion and conclusions**

297 GDI and PFI vehicles have different fuel injection technologies in their engines, which affects their emissions  
298 of gaseous and particulate pollutants. In GDI engine, the fuel is directly injected into cylinder, which benefits the  
299 fuel atomization and vaporization and provides better control of fuel volume and the combustion process (Liang et

300 al. 2013; Gao et al., 2015). Thus, in this study, the tested GDI vehicle has higher fuel economy and lower THC  
301 emission than the PFI vehicle. However, the insufficient mixing time allowed for the fuel and air leads to  
302 incomplete combustion in the GDI engine (Fu et al., 2014). In addition, direct fuel injection leads to fuel  
303 impingement onto surfaces of combustion chamber, where liquid pools form, favoring soot-like particulate  
304 formation (Ueberall et al., 2015; Chen et al., 2017). Consequently, larger particle mass and number are emitted by  
305 the GDI vehicle than from the PFI vehicle. The particles emitted by the GDI vehicle have higher EC mass fraction,  
306 leading to a lower OC/EC ratio. The considerable particle number emitted by gasoline vehicles, especially in GDI  
307 vehicles exhaust, makes a significant contribution to particle number concentration as well as seeds for further  
308 reactions in the atmosphere, and needs to be controlled in the future emission standards.

309 Our results show that the GDI vehicle contributes more to both primary and secondary aerosol than the PFI  
310 vehicle, and has greater impact on environment and air quality. In recent years, the market share of GDI vehicles  
311 exerts a continuous growth in China because they provide better fuel economy and lower CO<sub>2</sub> emissions. In 2016,  
312 GDI vehicles accounted for 25 % of China's market share in sales, and this proportion is expected to reach 60 %  
313 by 2020 (Wen et al., 2016). The PM enhancement of GDI vehicles with increasing population could potentially  
314 offset any PM emission reduction benefits, including the development of gasoline emission and fuel standards and  
315 the advanced engine technologies of gasoline vehicles. Therefore, our results highlight the necessity of further  
316 research and regulation of GDI vehicles.

317 It should be pointed out that the SOA formation factors in this study are based on one GDI vehicle and one  
318 PFI vehicle. Some previous studies proposed that vehicles have variations even though they meet similar  
319 specification vehicles and use the same fuel (Gordon et al., 2014; Jathar et al., 2014). Thus more researches with  
320 more vehicles for each technology are needed on SOA formation from vehicle exhaust.

321 Primary emissions and secondary organic formation from one GDI vehicle and one PFI vehicle were  
322 investigated when driving under cold-start BJC. The primary PM emitted by the GDI vehicle was 1.4 times greater  
323 than that from the PFI vehicle and the SOA formation from the GDI vehicle exhaust was 2.7 times greater than that  
324 from the PFI vehicle exhaust for the same OH exposure. The SOA production factors were  $54.77 \pm 10.70$  mg kg<sup>-1</sup>

325 fuel<sup>-1</sup> or 3.06±0.60 mg km<sup>-1</sup> for the GDI vehicle and 20.57±5.82 mg kg-fuel<sup>-1</sup> or 1.55±0.44 mg km<sup>-1</sup> for the PFI  
326 vehicle at an OH exposure of 5×10<sup>6</sup> molecular cm<sup>-3</sup> h, which is consistent with the values seen in previous studies.  
327 Considering the higher amounts of OA derived from primary emission and secondary formation, the GDI vehicle  
328 contribute considerably more to particle mass concentrations in the ambient air than the PFI vehicle.

329 The SOA formation was predicted from the gaseous precursors emitted by the GDI and PFI vehicles under  
330 high NO<sub>x</sub> condition. Single-ring aromatic VOCs could explain only 25-53 % of the measured SOA formation in  
331 the chamber experiments. The GDI vehicle exhibited higher fraction of unexplained SOA. More IVOCs and  
332 SVOCs were inferred as being emitted by the GDI vehicle.

333 With increasing population of GDI vehicles, any benefits of the aerosol emission reduction of gasoline  
334 vehicles are substantially offset, because GDI vehicles have significant contributions to ambient aerosols. More  
335 work is needed to improve the understanding of GDI vehicle emissions and to provide information for the  
336 regulation of gasoline vehicles.

337

338

339 *Data availability.* The data presented in this article are available from the authors upon request  
340 ([minhu@pku.edu.cn](mailto:minhu@pku.edu.cn)).

341

342

### 343 **Acknowledgments**

344 This work was supported by the National Basic Research Program of China (973 Program) (2013CB228503,  
345 2013CB228502), National Natural Science Foundation of China (91544214, 41421064, 51636003), the Strategic  
346 Priority Research Program of Chinese Academy of Sciences (XDB05010500), China Postdoctoral Science  
347 Foundation (2015M580929), and the National Science and Technology Support Program (2014BAC21B01). We  
348 also thank the State Key Lab of Automotive Safety and Energy at Tsinghua University for the support to  
349 experiments.





351 **Reference**

352 Alkidas, A. C.: Combustion advancements in gasoline engines, *Energy Conversion and Management*, 48, 2751-  
353 2761, 10.1016/j.enconman.2007.07.027, 2007.

354 Bahreini, R., Middlebrook, A. M., de Gouw, J. A., Warneke, C., Trainer, M., Brock, C. A., Stark, H., Brown, S. S.,  
355 Dube, W. P., Gilman, J. B., Hall, K., Holloway, J. S., Kuster, W. C., Perring, A. E., Prevot, A. S. H., Schwarz, J. P.,  
356 Spackman, J. R., Szidat, S., Wagner, N. L., Weber, R. J., Zotter, P., and Parrish, D. D.: Gasoline emissions dominate  
357 over diesel in formation of secondary organic aerosol mass, *Geophysical Research Letters*, 39,  
358 10.1029/2011gl050718, 2012.

359 Chen, L., Liang, Z., Zhang, X., and Shuai, S.: Characterizing particulate matter emissions from GDI and PFI  
360 vehicles under transient and cold start conditions, *Fuel*, 189, 131-140, 10.1016/j.fuel.2016.10.055, 2017.

361 DeCarlo, P. F., Kimmel, J. R., Trimborn, A., Northway, M. J., Jayne, J. T., Aiken, A. C., Gonin, M., Fuhrer, K.,  
362 Horvath, T., Docherty, K. S., Worsnop, D. R., and Jimenez, J. L.: Field-deployable, high-resolution, time-of-flight  
363 aerosol mass spectrometer, *Analytical Chemistry*, 78, 8281-8289, 10.1021/ac061249n, 2006.

364 Donahue, N. M., Robinson, A. L., Stanier, C. O., and Pandis, S. N.: Coupled partitioning, dilution, and chemical  
365 aging of semivolatile organics, *Environ. Sci. Technol.*, 40, 2635-2643, 10.1021/es052297c, 2006.

366 Du, Z., Hu, M., Peng, J., Guo, S., Zheng, R., Zheng, J., Shang, D., Qin, Y., Niu, H., Li, M., Yang, Y., Lu, S., Wu,  
367 Y., Shao, M., and Shuai, S.: Potential of secondary aerosol formation from Chinese gasoline engine exhaust, *Journal*  
368 *of environmental sciences (China)*, 66, 348-357, 10.1016/j.jes.2017.02.022, 2018.

369 Fu, H., Wang, Y., Li, X., and Shuai, S.: Impacts of Cold-Start and Gasoline RON on Particulate Emission from  
370 Vehicles Powered by GDI and PFI Engines, *SAE Technical Paper*, 2014-01-2836, 10.4271/2014-01-2836, 2014.

371 Gao, Z., Curran, S. J., Parks, J. E., II, Smith, D. E., Wagner, R. M., Daw, C. S., Edwards, K. D., and Thomas, J. F.:  
372 Drive cycle simulation of high efficiency combustions on fuel economy and exhaust properties in light-duty  
373 vehicles, *Applied Energy*, 157, 762-776, 10.1016/j.apenergy.2015.03.070, 2015.

374 Gentner, D. R., Jathar, S. H., Gordon, T. D., Bahreini, R., Day, D. A., El Haddad, I., Hayes, P. L., Pieber, S. M.,  
375 Platt, S. M., de Gouw, J., Goldstein, A. H., Harley, R. A., Jimenez, J. L., Prevot, A. S. H., and Robinson, A. L.:

376 Review of Urban Secondary Organic Aerosol Formation from Gasoline and Diesel Motor Vehicle Emissions,  
377 Environmental science & technology, 51, 1074-1093, 10.1021/acs.est.6b04509, 2017.

378 Gordon, T. D., Presto, A. A., May, A. A., Nguyen, N. T., Lipsky, E. M., Donahue, N. M., Gutierrez, A., Zhang, M.,  
379 Maddox, C., Rieger, P., Chattopadhyay, S., Maldonado, H., Maricq, M. M., and Robinson, A. L.: Secondary organic  
380 aerosol formation exceeds primary particulate matter emissions for light-duty gasoline vehicles, Atmos. Chem.  
381 Phys. , 14, 4661-4678, 10.5194/acp-14-4661-2014, 2014.

382 Guo, S., Hu, M., Zamora, M. L., Peng, J., Shang, D., Zheng, J., Du, Z., Wu, Z., Shao, M., Zeng, L., Molina, M. J.,  
383 and Zhang, R.: Elucidating severe urban haze formation in China, Proceedings of the National Academy of  
384 Sciences of the United States of America, 111, 17373-17378, 10.1073/pnas.1419604111, 2014.

385 Hayes, P. L., Ortega, A. M., Cubison, M. J., Froyd, K. D., Zhao, Y., Cliff, S. S., Hu, W. W., Toohey, D. W., Flynn,  
386 J. H., Lefer, B. L., Grossberg, N., Alvarez, S., Rappenglueck, B., Taylor, J. W., Allan, J. D., Holloway, J. S., Gilman,  
387 J. B., Kuster, W. C., De Gouw, J. A., Massoli, P., Zhang, X., Liu, J., Weber, R. J., Corrigan, A. L., Russell, L. M.,  
388 Isaacman, G., Worton, D. R., Kreisberg, N. M., Goldstein, A. H., Thalman, R., Waxman, E. M., Volkamer, R., Lin,  
389 Y. H., Surratt, J. D., Kleindienst, T. E., Offenberg, J. H., Dusanter, S., Griffith, S., Stevens, P. S., Brioude, J.,  
390 Angevine, W. M., and Jimenez, J. L.: Organic aerosol composition and sources in Pasadena, California, during the  
391 2010 CalNex campaign, Journal of Geophysical Research-Atmospheres, 118, 9233-9257, 10.1002/jgrd.50530,  
392 2013.

393 Hays, M. D., Preston, W., George, B. J., Schmid, J., Baldauf, R., Snow, R., Robinson, J. R., Long, T., and Faircloth,  
394 J.: Carbonaceous aerosols emitted from light-duty vehicles operating on gasoline and ethanol fuel blends,  
395 Environmental science & technology, 47, 14502-14509, 10.1021/es403096v, 2013.

396 Hu, W., Hu, M., Hu, W., Jimenez, J. L., Yuan, B., Chen, W., Wang, M., Wu, Y., Chen, C., Wang, Z., Peng, J., Zeng,  
397 L., and Shao, M.: Chemical composition, sources, and aging process of submicron aerosols in Beijing: Contrast  
398 between summer and winter, Journal of Geophysical Research-Atmospheres, 121, 1955-1977,  
399 10.1002/2015jd024020, 2016.

400 Huang, R.-J., Zhang, Y., Bozzetti, C., Ho, K.-F., Cao, J.-J., Han, Y., Daellenbach, K. R., Slowik, J. G., Platt, S. M.,  
401 Canonaco, F., Zotter, P., Wolf, R., Pieber, S. M., Bruns, E. A., Crippa, M., Ciarelli, G., Piazzalunga, A.,  
402 Schwikowski, M., Abbaszade, G., Schnelle-Kreis, J., Zimmermann, R., An, Z., Szidat, S., Baltensperger, U.,  
403 Haddad, I. E., and Prévôt, A. S. H.: High secondary aerosol contribution to particulate pollution during haze events  
404 in China, *Nature*, 10.1038/nature13774, 2014.

405 Ito, Y., Shimoda, T., Aoki, T., Yuuki, K., Sakamoto, H., Kato, K., Their, D., Kattouah, P., Ohara, E. and Vogt, C.:  
406 Next Generation of Ceramic Wall Flow Gasoline Particulate Filter with Integrated Three Way Catalyst, SAE  
407 Technical Paper 2015-01-1073, 2015, doi:10.4271/2015-01-1073, 2015.

408 Jathar, S. H., Gordon, T. D., Hennigan, C. J., Pye, H. O. T., Pouliot, G., Adams, P. J., Donahue, N. M., and Robinson,  
409 A. L.: Unspeciated organic emissions from combustion sources and their influence on the secondary organic aerosol  
410 budget in the United States, *Proc. Natl. Acad. Sci. USA*, 111, 10473-10478, 10.1073/pnas.1323740111, 2014.

411 Jathar, S. H., Woody, M., Pye, H. O. T., Baker, K. R., and Robinson, A. L.: Chemical transport model simulations  
412 of organic aerosol in southern California: model evaluation and gasoline and diesel source contributions,  
413 *Atmospheric Chemistry and Physics*, 17, 4305-4318, 10.5194/acp-17-4305-2017, 2017.

414 Kamal, A., Cincinelli, A., Martellini, T., and Malik, R. N.: A review of PAH exposure from the combustion of  
415 biomass fuel and their less surveyed effect on the blood parameters, *Environmental Science and Pollution Research*,  
416 22, 4076-4098, 10.1007/s11356-014-3748-0, 2015.

417 Kanakidou, M., Seinfeld, J. H., Pandis, S. N., Barnes, I., Dentener, F. J., Facchini, M. C., Van Dingenen, R., Ervens,  
418 B., Nenes, A., Nielsen, C. J., Swietlicki, E., Putaud, J. P., Balkanski, Y., Fuzzi, S., Horth, J., Moortgat, G. K.,  
419 Winterhalter, R., Myhre, C. E. L., Tsigaridis, K., Vignati, E., Stephanou, E. G., and Wilson, J.: Organic aerosol and  
420 global climate modelling: a review, *Atmospheric Chemistry and Physics*, 5, 1053-1123, 2005.

421 Kramp, F., and Paulson, S. E.: On the uncertainties in the rate coefficients for OH reactions with hydrocarbons, and  
422 the rate coefficients of the 1,3,5-trimethylbenzene and m-xylene reactions with OH radicals in the gas phase,  
423 *Journal of Physical Chemistry A*, 102, 2685-2690, 10.1021/jp973289o, 1998.

424 Li, M., Hu, M., Wu, Y., Qin, Y., Zheng, R., Peng, J., Guo, Q., Xiao, Y., Hu, W., Zheng, J., Du, Z., Xiao, J., Shuai,  
425 S.: Characteristics of Particulate Organic Matters Emissions from Gasoline Direct Injection Engine and Its  
426 Influence Factors, *Proceedings of the Chinese Society of Electrical Engineering*, 36, 4443-4451.

427 Liang, B., Ge, Y., Tan, J., Han, X., Gao, L., Hao, L., Ye, W., and Dai, P.: Comparison of PM emissions from a  
428 gasoline direct injected (GDI) vehicle and a port fuel injected (PFI) vehicle measured by electrical low pressure  
429 impactor (ELPI) with two fuels: Gasoline and M15 methanol gasoline, *Journal of Aerosol Science*, 57, 22-31,  
430 10.1016/j.jaerosci.2012.11.008, 2013.

431 Lindinger, W., Hansel, A., and Jordan, A.: On-line monitoring of volatile organic compounds at pptv levels by  
432 means of proton-transfer-reaction mass spectrometry (PTR-MS) - Medical applications, food control and  
433 environmental research, *International Journal of Mass Spectrometry*, 173, 191-241, 10.1016/s0168-  
434 1176(97)00281-4, 1998.

435 Liu, T., Wang, X., Deng, W., Hu, Q., Ding, X., Zhang, Y., He, Q., Zhang, Z., Lü, S., Bi, X., Chen, J., and Yu, J.:  
436 Secondary organic aerosol formation from photochemical aging of light-duty gasoline vehicle exhausts in a smog  
437 chamber, *Atmos. Chem. Phys.*, 15, 9049-9062, 10.5194/acp-15-9049-2015, 2015.

438 Lu, K. D., Hofzumahaus, A., Holland, F., Bohn, B., Brauers, T., Fuchs, H., Hu, M., Häeler, R., Kita, K., Kondo,  
439 Y., Li, X., Lou, S. R., Oebel, A., Shao, M., Zeng, L. M., Wahner, A., Zhu, T., Zhang, Y. H., and Rohrer, F.: Missing  
440 OH source in a suburban environment near Beijing: observed and modelled OH and HO<sub>2</sub>  
441 concentrations in summer 2006, *Atmos. Chem. Phys.*, 13, 1057-1080, 10.5194/acp-13-1057-2013, 2013.

442 **Maria, S. F., Russell, L. M., Gilles, M. K., and Myneni, S. C. B.: Organic aerosol growth mechanisms and their  
443 climate-forcing implications, *Science*, 306, 1921-1924, 10.1126/science.1103491, 2004.**

444 Maricq, M. M., Podsiadlik, D. H., and Chase, R. E.: Gasoline vehicle particle size distributions: Comparison of  
445 steady state, FTP, and US06 measurements, *Environmental science & technology*, 33, 2007-2015,  
446 10.1021/es981005n, 1999.

447 Mathis, U., Mohr, M., and Forss, A. M.: Comprehensive particle characterization of modern gasoline and diesel  
448 passenger cars at low ambient temperatures, *Atmospheric Environment*, 39, 107-117,  
449 10.1016/j.atmosenv.2004.09.029, 2005.

450 May, A. A., Nguyen, N. T., Presto, A. A., Gordon, T. D., Lipsky, E. M., Karve, M., Gutierrez, A., Robertson, W. H.,  
451 Zhang, M., Brandow, C., Chang, O., Chen, S., Cicero-Fernandez, P., Dinkins, L., Fuentes, M., Huang, S.-M., Ling,  
452 R., Long, J., Maddox, C., Massetti, J., McCauley, E., Miguel, A., Na, K., Ong, R., Pang, Y., Rieger, P., Sax, T., Tin,  
453 T., Thu, V., Chattopadhyay, S., Maldonado, H., Maricq, M. M., and Robinson, A. L.: Gas- and particle-phase  
454 primary emissions from in-use, on-road gasoline and diesel vehicles, *Atmospheric Environment*, 88, 247-260,  
455 10.1016/j.atmosenv.2014.01.046, 2014.

456 Myung, C.-L., Kim, J., Choi, K., Hwang, I. G., and Park, S.: Comparative study of engine control strategies for  
457 particulate emissions from direct injection light-duty vehicle fueled with gasoline and liquid phase liquefied  
458 petroleum gas (LPG), *Fuel*, 94, 348-355, 10.1016/j.fuel.2011.10.041, 2012.

459 Ng, N. L., Kroll, J. H., Chan, A. W. H., Chhabra, P. S., Flagan, R. C., and Seinfeld, J. H.: Secondary organic aerosol  
460 formation from m-xylene, toluene, and benzene, *Atmos. Chem. Phys.*, 7, 3909–3922, 2007.

461 Nordin, E. Z., Eriksson, A. C., Roldin, P., Nilsson, P. T., Carlsson, J. E., Kajos, M. K., Hellén, H., Wittbom, C.,  
462 Rissler, J., Löndahl, J., Swietlicki, E., Svenningsson, B., Bohgard, M., Kulmala, M., Hallquist, M., and Pagels, J.  
463 H.: Secondary organic aerosol formation from idling gasoline passenger vehicle emissions investigated in a smog  
464 chamber, *Atmos. Chem. Phys.*, 13, 6101-6116, 10.5194/acp-13-6101-2013, 2013.

465 Odum, J. R., Hoffmann, T., Bowman, F., Collins, D., Flagan, R. C., and Seinfeld, J. H.: Gas/particle partitioning  
466 and secondary organic aerosol yields, *Environ. Sci. Technol.*, 30, 2580-2585, 10.1021/es950943+, 1996.

467 Peng, J., Hu, M., Du, Z., Wang, Y., Zheng, J., Zhang, W., Yang, Y., Qin, Y., Zheng, R., Xiao, Y., Wu, Y., Lu, S., Wu,  
468 Z., Guo, S., Mao, H., and Shuai, S.: Gasoline aromatic: a critical determinant of urban secondary organic aerosol  
469 formation, *Atmospheric Chemistry and Physics*, 2017, in press.

470 Platt, S. M., El Haddad, I., Zardini, A. A., Clairotte, M., Astorga, C., Wolf, R., Slowik, J. G., Temime-Roussel, B.,  
471 Marchand, N., Ježek, I., Drinovec, L., Močnik, G., Möhler, O., Richter, R., Barmet, P., Bianchi, F., Baltensperger,

472 U., and Prévôt, A. S. H.: Secondary organic aerosol formation from gasoline vehicle emissions in a new mobile  
473 environmental reaction chamber, *Atmos. Chem. Phys.*, 13, 9141-9158, 10.5194/acp-13-9141-2013, 2013.

474 Robinson, A. L., Donahue, N. M., Shrivastava, M. K., Weitkamp, E. A., Sage, A. M., Grieshop, A. P., Lane, T. E.,  
475 Pierce, J. R., and Pandis, S. N.: Rethinking organic aerosols: Semivolatile emissions and photochemical aging,  
476 *Science*, 315, 1259-1262, 10.1126/science.1133061, 2007.

477 Saliba, G., Saleh, R., Zhao, Y., Presto, A. A., Lambe, A. T., Frodin, B., Sardar, S., Maldonado, H., Maddox, C.,  
478 May, A. A., Drozd, G. T., Goldstein, A. H., Russell, L. M., Hagen, F., and Robinson, A. L.: Comparison of Gasoline  
479 Direct-Injection (GDI) and Port Fuel Injection (PFI) Vehicle Emissions: Emission Certification Standards, Cold-  
480 Start, Secondary Organic Aerosol Formation Potential, and Potential Climate Impacts, *Environmental science &*  
481 *technology*, 51, 6542-6552, 10.1021/acs.est.6b06509, 2017.

482 Schauer, J. J., Kleeman, M. J., Cass, G. R. and Simoneit, B. R. T.: Measurement of Emissions from Air Pollution  
483 Sources. 5. C1-C32 Organic Compounds from Gasoline-Powered Motor Vehicles, *Environmental science &*  
484 *technology*, 36, 1169-1180, 2002.

485 Seinfeld, J. H., Kleindienst, T. E., Edney, E. O., and Cohen, J. B.: Aerosol growth in a steady-state, continuous flow  
486 chamber: Application to studies of secondary aerosol formation, *Aerosol Science and Technology*, 37, 728-734,  
487 10.1080/02786820390214954, 2003.

488 Song, C., Na, K. S., and Cocker, D. R.: Impact of the hydrocarbon to NO<sub>x</sub> ratio on secondary organic aerosol  
489 formation, *Environ. Sci. Technol.*, 39, 3143-3149, 10.1021/es0493244, 2005.

490 Ueberall, A., Otte, R., Eilts, P., and Krahl, J.: A literature research about particle emissions from engines with direct  
491 gasoline injection and the potential to reduce these emissions, *Fuel*, 147, 203-207, 10.1016/j.fuel.2015.01.012,  
492 2015.

493 Wang, Y., Zheng, R., Qin, Y., Peng, J., Li, M., Lei, J., Wu, Y., Hu, M., and Shuai, S.: The impact of fuel compositions  
494 on the particulate emissions of direct injection gasoline engine, *Fuel*, 166, 543-552, 10.1016/j.fuel.2015.11.019,  
495 2016.

496 Wang, Z. B., Hu, M., Wu, Z. J., Yue, D. L., He, L. Y., Huang, X. F., Liu, X. G., and Wiedensohler, A.: Long-term  
497 measurements of particle number size distributions and the relationships with air mass history and source  
498 apportionment in the summer of Beijing, *Atmospheric Chemistry and Physics*, 13, 10159-10170, 10.5194/acp-13-  
499 10159-2013, 2013.

500 Wen, Y., Wang, Y., Fu, C., Deng, W., Zhan, Z., Tang, Y., Li, X., Ding, H., and Shuai, S.: The Impact of Injector  
501 Deposits on Spray and Particulate Emission of Advanced Gasoline Direct Injection Vehicle, SAE Technical Paper,  
502 2016-01-2284, 10.4271/2016-01-2284, 2016.

503 Yang, B., Ma, P. K., Shu, J. N., Zhang, P., Huang, J. Y. and Zhang, H. X.: Formation mechanism of secondary  
504 organic aerosol from ozonolysis of gasoline vehicle exhaust, *Environmental Pollution*, 234, 960-968,  
505 10.1016/j.envpol.2017.12.048, 2018.

506 Yuan, B., Shao, M., de Gouw, J., Parrish, D. D., Lu, S., Wang, M., Zeng, L., Zhang, Q., Song, Y., Zhang, J., and  
507 Hu, M.: Volatile organic compounds (VOCs) in urban air: How chemistry affects the interpretation of positive  
508 matrix factorization (PMF) analysis, *Journal of Geophysical Research: Atmospheres*, 117, n/a-n/a,  
509 10.1029/2012jd018236, 2012.

510 Zhang, Q., Jimenez, J. L., Canagaratna, M. R., Allan, J. D., Coe, H., Ulbrich, I., Alfarra, M. R., Takami, A.,  
511 Middlebrook, A. M., Sun, Y. L., Dzepina, K., Dunlea, E., Docherty, K., DeCarlo, P. F., Salcedo, D., Onasch, T.,  
512 Jayne, J. T., Miyoshi, T., Shimojo, A., Hatakeyama, S., Takegawa, N., Kondo, Y., Schneider, J., Drewnick, F.,  
513 Borrmann, S., Weimer, S., Demerjian, K., Williams, P., Bower, K., Bahreini, R., Cottrell, L., Griffin, R. J.,  
514 Rautiainen, J., Sun, J. Y., Zhang, Y. M., and Worsnop, D. R.: Ubiquity and dominance of oxygenated species in  
515 organic aerosols in anthropogenically-influenced Northern Hemisphere midlatitudes, *Geophysical Research Letters*,  
516 34, 10.1029/2007gl029979, 2007.

517 Zhang, X., Cappa, C. D., Jathar, S. H., McVay, R. C., Ensberg, J. J., Kleeman, M. J., and Seinfeld, J. H.: Influence  
518 of vapor wall loss in laboratory chambers on yields of secondary organic aerosol, *Proc. Natl. Acad. Sci. USA*, 111,  
519 5802-5807, 10.1073/pnas.1404727111, 2014.



520 Zhao, B., Wang, S., Donahue, N. M., Jathar, S. H., Huang, X., Wu, W., Hao, J., and Robinson, A. L.: Quantifying  
521 the effect of organic aerosol aging and intermediate-volatility emissions on regional-scale aerosol pollution in  
522 China, *Scientific Reports*, 6, 10.1038/srep28815, 2016.

523 Zhao, Y., Nguyen, N. T., Presto, A. A., Hennigan, C. J., May, A. A., and Robinson, A. L.: Intermediate Volatility  
524 Organic Compound Emissions from On-Road Gasoline Vehicles and Small Off-Road Gasoline Engines,  
525 *Environmental science & technology*, 50, 4554-4563, 10.1021/acs.est.5b06247, 2016.

526 Zhao, Y., Saleh, R., Saliba, G., Presto, A. A., Gordon, T. D., Drozd, G. T., Goldstein, A. H., Donahue, N. M., and  
527 Robinson, A. L.: Reducing secondary organic aerosol formation from gasoline vehicle exhaust, *Proceedings of the*  
528 *National Academy of Sciences of the United States of America*, 114, 6984-6989, 10.1073/pnas.1620911114, 2017.

529 Zhu, R., Hu, J., Bao, X., He, L., Lai, Y., Zu, L., Li, Y., and Su, S.: Tailpipe emissions from gasoline direct injection  
530 (GDI) and port fuel injection (PFI) vehicles at both low and high ambient temperatures, *Environmental Pollution*,  
531 216, 223-234, 10.1016/j.envpol.2016.05.066, 2016.

532 Zimmerman, N., Wang, J. M., Jeong, C.-H., Ramos, M., Hilker, N., Healy, R. M., Sabaliauskas, K., Wallace, J. S.,  
533 and Evans, G. J.: Field Measurements of Gasoline Direct Injection Emission Factors: Spatial and Seasonal  
534 Variability, *Environmental science & technology*, 50, 2035-2043, 10.1021/acs.est.5b04444, 2016.

535

536 Table 1 Descriptions of the gasoline direct injection (GDI) and port fuel injection (PFI) vehicles used in the  
537 experiments.

Vehicle	Make and model	Emission standard class	Model year	Mileage (km)	Displacement (cm <sup>3</sup> )	Power (kW)	Weight (kg)
GDI	VW Sagitar	China V	2015	3000	1395	110	1395
PFI	Honda Civic	China IV	2009	42500	1799	103	1280

538

539 Table 2 Overview of all instruments used to measure the gas and particulate phase pollutants in the experiments.

Parameter	Phase	Instrument	Note
CO, CO <sub>2</sub> , NO <sub>x</sub> and total hydrocarbon (THC) concentration	Gas	Gas analyzer AVL Emissions Bench II	On-line
Aerosol number size distribution	Particle	DMS500	On-line
PM <sub>2.5</sub>	Particle	Balance (AX105DR)	Off-line
Organic carbon/Elemental carbon concentration	Particle	OC/EC analyzer	Off-line
CO concentration	Gas	48i CO analyzer	On-line
NO, NO <sub>2</sub> , and NO <sub>x</sub> concentration	Gas	42i NO-NO <sub>2</sub> -NO <sub>x</sub> analyzer	On-line
O <sub>3</sub> concentration	Gas	49i O <sub>3</sub> analyzer	On-line
VOCs concentration	Gas	Proton transfer reaction mass spectrometer (PTR-MS)	On-line
Aerosol number (mass) size distribution	Particle	Scanning mobility particle sizer (SMPS, consist of 3081-DMA and 3775-CPC),	On-line
Size resolved non-refractory aerosol	Particle	High resolution time-of-flight aerosol mass spectrometer (HR-ToF-AMS)	On-line

540

541

542 Table 3 Emission factors (EFs) of gaseous pollutants from the gasoline direct injection (GDI) and port fuel injection (PFI) vehicles in  
 543 this study and those of previous studies.

	This study				Saliba et al., 2017		May et al., 2014	Platt et al., 2013		Zhu et al., 2016	
	GDI		PFI		GDI	PFI	PFI <sup>a</sup>			GDI	PFI
	China V		China IV		ULEV	ULEV	LEV II	Euro V		China IV	China IV
	Cold BJC				Cold UC <sup>b</sup>		Cold UC	Cold NEDC		Cold WLTC <sup>c</sup>	
	g kg- fuel <sup>-1</sup>	g km <sup>-1</sup>	g kg- fuel <sup>-1</sup>	g km <sup>-1</sup>	g km <sup>-1</sup>	g km <sup>-1</sup>	g kg-fuel <sup>-1</sup>	g kg-fuel <sup>-1</sup>	g km <sup>-1</sup>	g km <sup>-1</sup>	g km <sup>-1</sup>
CO <sub>2</sub>	3439 ±23	213 ±4	3350 ±24	283 ±4	-	-	-	-	-	187	215
THC	1.55 ±0.22	0.09 ±0.01	1.70 ±0.19	0.13 ±0.01	0.02	0.06	0.64	0.91-1.06	0.036- 0.042	0.05	0.03
Benzene	0.056 ±0.011	0.003 ±0.001	0.061 ±0.016	0.005 ±0.001	-	-	0.018	-	0.002	-	-
Toluene	0.101 ±0.004	0.006 ±0.001	0.220 ±0.047	0.017 ±0.004	-	-	0.026	-	0.002	-	-

544 <sup>a</sup> 22 PFI vehicles and 3 GDI vehicles;

545 <sup>b</sup> UC: Unified Cycle;

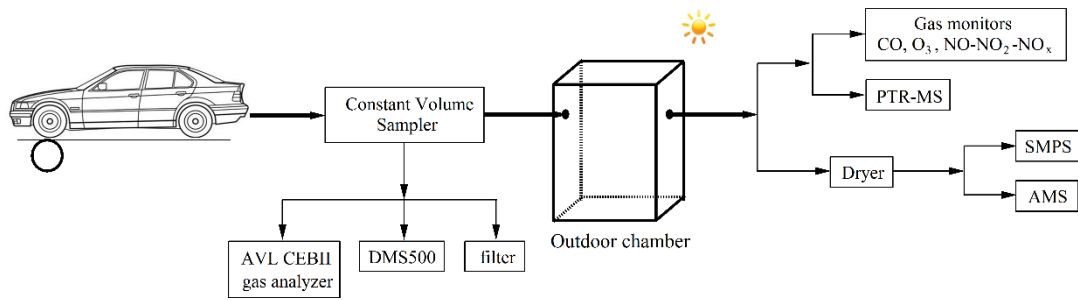
546 <sup>c</sup> WLTC: Worldwide-harmonized Light-duty Test Cycle

547 Table 4 EFs of primary aerosols, including carbonaceous aerosols and particulate polycyclic aromatic hydrocarbons (PAHs) from the  
 548 GDI and PFI vehicles in this study and those of previous studies.

	This study				Saliba et al., 2017		May et al., 2014	Platt et al., 2013		Zhu et al., 2016	
	GDI		PFI		GDI	PFI	PFI			GDI	PFI
	China V		China IV		ULEV	ULEV	LEV II	Euro V		China IV	China IV
	Cold BJC				Cold UC		Cold UC	Cold NEDC		Cold WLTC	
	mg kg- fuel <sup>-1</sup>	mg km <sup>-1</sup>	mg kg- fuel <sup>-1</sup>	mg km <sup>-1</sup>	mg km <sup>-1</sup>	mg km <sup>-1</sup>	mg kg-fuel <sup>-1</sup>	mg kg- fuel <sup>-1</sup>	mg km <sup>-1</sup>	mg km <sup>-1</sup>	mg km <sup>-1</sup>
PM <sub>2.5</sub>	61.7±24.5	3.4±1.4	33.4±25.6	2.5±1.9	3.9	2.4	18.0	-	-	1.5	1.0
EC	10.7±3.6	0.6±0.2	2.4±1.6	0.2±0.1	3.0	0.6	12.2	11.2-20.0	1.2-1.7	-	-
POA	41.7±9.8	2.3±0.6	25.0±0.3	1.9±0.1	0.4	0.6	5.2	24.5-19.7	0.4-1.4	-	-
OC/EC	3.2		8.7		0.1	0.8	0.4	0.2-1.8		-	-
PAHs(×10 <sup>6</sup> )	20.4±2.1	1.1±0.1	13.2±4.1	1.0±0.3	-	-	-	-	-	-	-

549

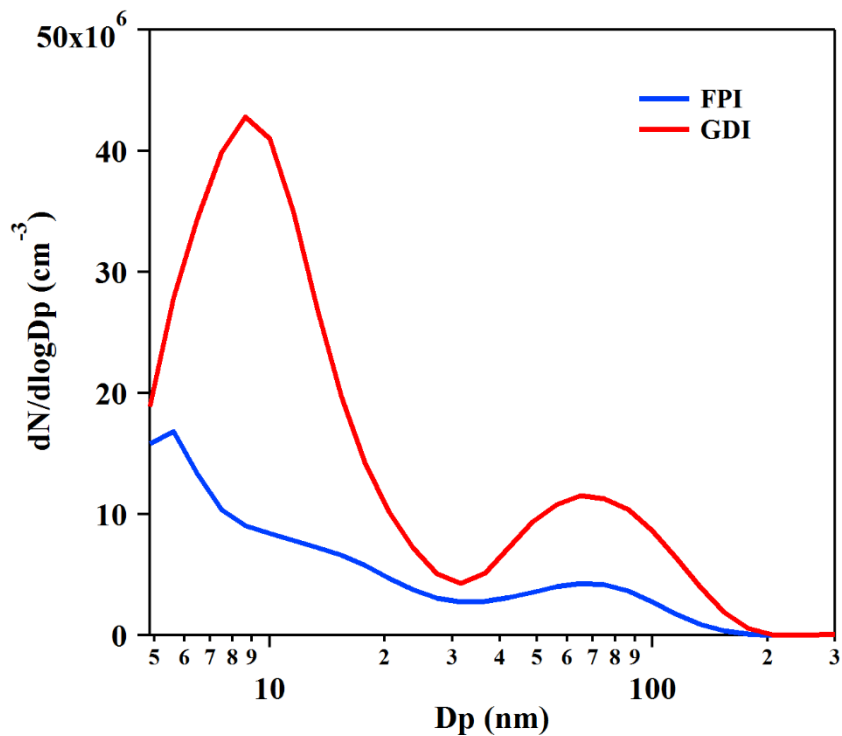
550



551

552 Figure 1. Schematic diagram of the outdoor chamber set up for the experiments.

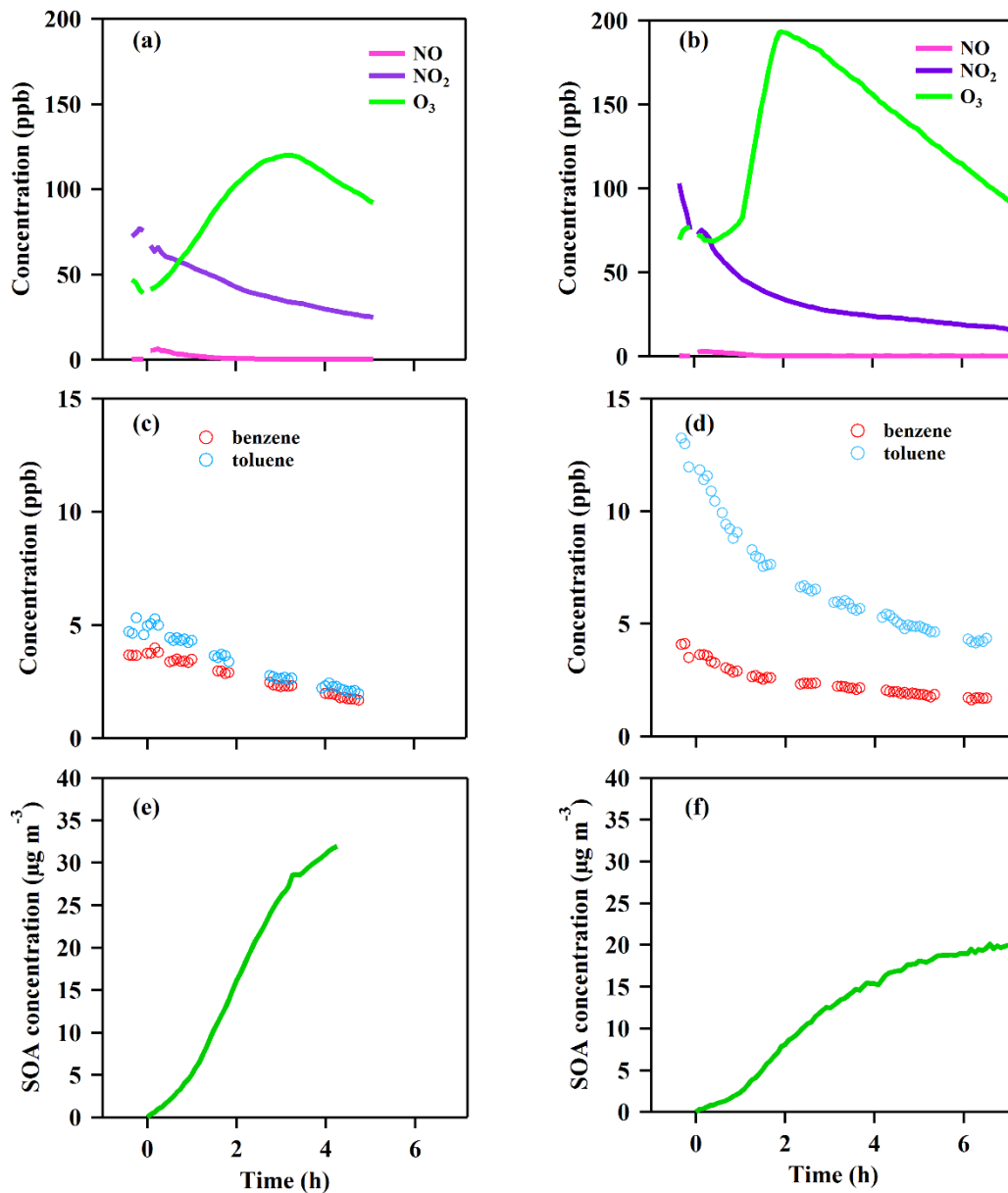
553



554

555 Figure 2. Number size distributions of primary PM emitted from the GDI (red line) and PFI (blue line) gasoline  
 556 vehicles. The results are average of particle number emissions from vehicles during a whole BJC, measured by  
 557 DMS500 in the CVS system. The particles were heated to 150°C in the DMS500.

558



559

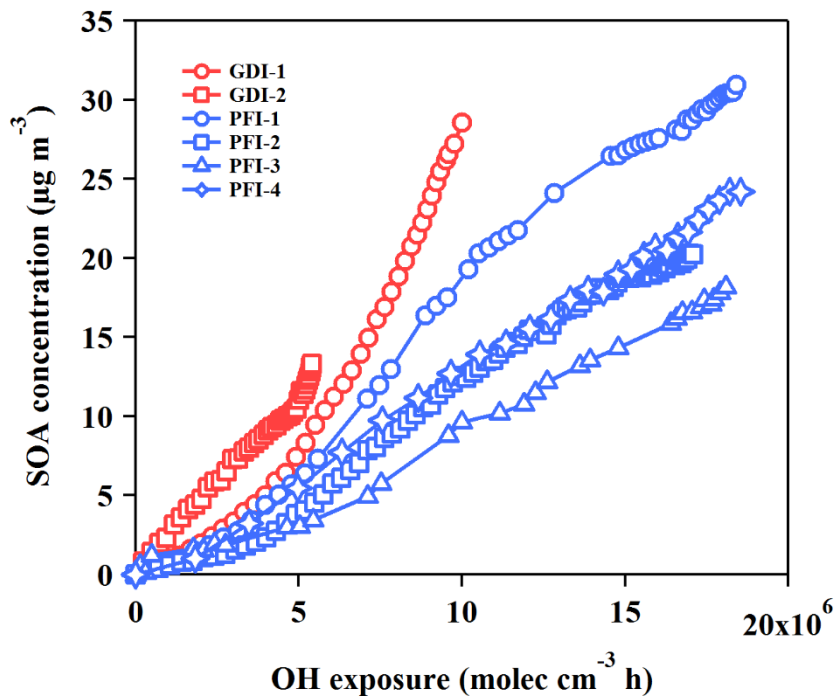
560 Figure 3. Time series of the gases and particle evolutions over the photochemical age in the chamber experiments

561 from the GDI vehicle exhaust (a, c, e) and PFI vehicle exhaust (b, d, f). (a, b): NO, NO<sub>2</sub> and O<sub>3</sub> concentration; (c,

562 d): benzene and toluene concentration; (e, f): corrected SOA concentration.

563



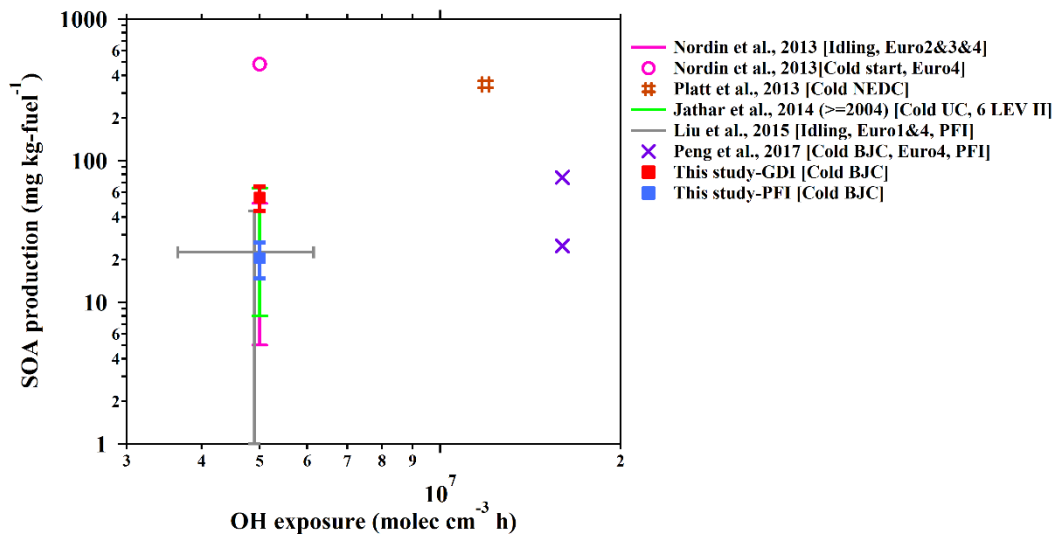


564

565 Figure 4. SOA productions from the GDI vehicle exhaust (red markers) and the PFI vehicle exhaust (blue markers)

566 as functions of OH exposure in the chamber experiments.

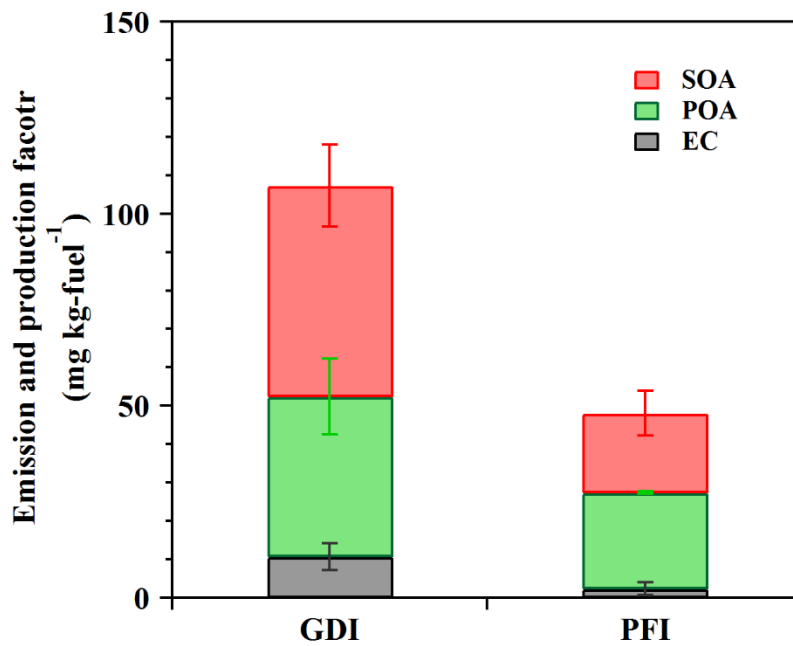
567



568

569 Figure 5. Fuel-based SOA production from gasoline vehicle exhaust as a function of OH exposure in the chamber  
 570 simulations. The SOA production data are from published studies of chamber simulation of gasoline vehicle  
 571 exhaust. From the study of Jathar et al. (2014), the SOA production of vehicles manufactured in 2004 or later (LEV  
 572 II) is selected, which is a model year that is more close to those of the vehicles in this study. The error bars of  
 573 previous results indicate the range of OH exposure (x axis) and SOA production (y axis) in their simulations. The  
 574 driving cycles and vehicle information are also noted in the legend of each study.

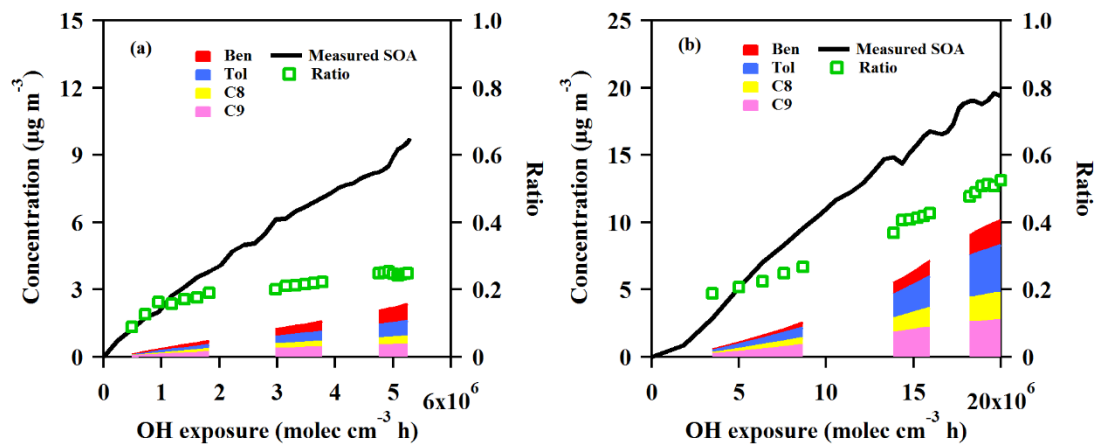
575



576

577 Figure 6 EC and POA EFs as well as corrected SOA production factors from the GDI and PFI vehicle exhausts in  
 578 this study (OH exposure =  $5 \times 10^6$  molecular  $\text{cm}^{-3}$  h).

579



580

581 Figure 7. Measured and predicted SOA concentration as a function of OH exposure from GDI vehicle exhaust (a)  
 582 and PFI vehicle exhaust (b) in the chamber experiments. The black line is the measured SOA concentration with  
 583 wall-loss and particle dilution correction during the experiment. The red, blue, yellow and pink areas are predicted  
 584 SOA concentration estimated from benzene, toluene, C8 alkylbenzene and C9 alkylbenzene, respectively. The  
 585 green markers are the ratios of the predicted SOA to the measured SOA.

586